

## **GACP Progress Report, FY 2001**

**PI:** Cora E. Randall

**Address:**

University of Colorado, Laboratory for Atmospheric and Space Physics, Boulder, CO 80309.

*email:* randall@lasp.colorado.edu

*tel:* (303) 492-8208

*fax:* (303) 492-6946

**CoIs:** Mike Callan, Frank Eparvier, Dave Rusch, and R. Todd Clancy

**Title:** Solar Mesosphere Explorer Measurements of El Chichón Aerosols

**Proposal Abstract:**

We were funded to “resurrect” data from the Solar Mesosphere Explorer (SME) in order to provide the climate community with information regarding stratospheric aerosol forcing after the eruption of the El Chichón volcano in 1982. The database provided by this proposal will enable climate modelers to subtract stratospheric aerosol effects from column measurements in order to define the tropospheric aerosol contribution after the El Chichón eruption. The goal is to provide the climate community with the optical depth of aerosols in the visible, near infrared and thermal infrared spectral regions. Specifically, SME radiance data from the 0.44, 1.27, 1.87, and 6.8  $\mu\text{m}$  channels will be used. We proposed to improve on previously published retrieval techniques in order to extract and publish extinction and size distribution information over more extended spatial and temporal regimes than previously possible.

**Objectives:**

To understand and predict global climate change, it is necessary to accurately assess the radiative forcing caused by atmospheric aerosols. Of the natural radiative forcings, injections of aerosols into the stratosphere by volcanic eruptions are the most significant with regard to the global radiation balance. The overall purpose of this program is to extend the satellite measurements of global stratospheric aerosol profiles back in time to the eruption of El Chichón in 1982, using SME data. SME made global measurements of aerosols from several months prior to the eruption of El Chichón through 1986. The SME radiance data are being inverted to calculate aerosol extinction profiles at 0.44, 1.27, 1.87 and 6.8  $\mu\text{m}$ . These profiles and the total vertical

optical depths derived from them will be provided to the climate community for input to global models.

**Approach:**

The approach is to modify existing codes [Eparvier *et al.*, 1994] to develop new algorithms for calculating aerosol extinction at the four SME aerosol wavelengths. Previously, aerosol extinction profiles and vertical optical depths at 6.8  $\mu\text{m}$  were calculated from the SME data, but with limited temporal and spatial resolution and coverage. Proposed improvements to the new inversion codes include reducing the amount of radiance profile binning, to improve the temporal and spatial resolution of the derived extinction profiles. The intent is also to use a water vapor climatology for subtraction of the water vapor component in the 6.8  $\mu\text{m}$  channel, to allow calculations of extinction beyond late 1984 (the limit of previous work). In previous work [Eparvier *et al.*, 1994], aerosol extinction profiles were not calculated at wavelengths of 0.44, 1.27 and 1.87  $\mu\text{m}$ . This is because the goal of that work was to produce size distribution parameters, and this was possible without completing a full inversion of the data. The approach here is to invert the slant path radiance profiles to obtain profiles of the phase-modulated extinction coefficients. Assumptions for size distribution parameters (and thus the scattering phase function) based on the work of Eparvier *et al.* will then be used to calculate the aerosol extinction profiles and vertical optical depths in all channels. Other improvements to the algorithms include using NCEP data to model the Rayleigh contribution to the near-IR radiance profiles, rather than climatological temperatures.

## Third Year Progress Report

### A. Summary of First Year Progress

During the first year of the proposed work, the 6.8- $\mu\text{m}$  retrieval algorithms were improved, and all data were inverted with the new algorithms to generate extinction profiles. The most significant improvements were inversions on an event-by-event basis (instead of calculating only weekly, and thus zonally averaged, profiles), and a significantly more accurate water vapor subtraction scheme [Callan *et al.*, 1999]. These profiles are available to other team members. Also during the first year, preliminary algorithms were developed for calculating extinction profiles at 1.27 and 1.87  $\mu\text{m}$ .

### B. Summary of Second Year Progress

During the second year of the proposed work, our major accomplishment was to recognize and correct unexpected errors in the altitude registration of the original SME 1.27 and 1.87  $\mu\text{m}$  merged radiance profiles. These errors affected all SME profiles at 1.27 and 1.87  $\mu\text{m}$ , and also affected SME data in the UV (265 nm); thus their correction was necessary both for the GACP program and for other programs (e.g., polar mesospheric cloud studies) that utilize the SME data. Also, as part of the SME archival effort, we began to transfer all of the SME data from old 9-track tapes to online media. Preliminary validation of the SME 1.27  $\mu\text{m}$  extinctions began with collection and organization of correlative data.

### C. Third Year Progress

During the third year, we optimized the 1.27 and 1.87  $\mu\text{m}$  inversion algorithms, and applied them to all of the corrected SME radiance profiles to generate phase-modulated extinction coefficients. The algorithm optimization focused primarily on four items: (1) refining the subtraction of the  $\text{O}_2(^1\Delta_g)$  contribution to the 1.27- $\mu\text{m}$  radiances, (2) incorporating the instrument field-of-view (fov) function, (3) including effects of atmospheric refraction in the forward model, and (4) achieving internal consistency by implementing an approach using weighted least squares with smoothness constraints.

The radiance at 1.27 and 1.87  $\mu\text{m}$  due to scattering by aerosols can be expressed as:

$$R_{aer}(\mathbf{I}) = F(\mathbf{I})\Delta\mathbf{I} \int_{LOS} \mathbf{b}_{aer}(\mathbf{I}, s)P(\mathbf{I}, \mathbf{J}, s)ds \quad (1)$$

where  $F(\mathbf{I})$  is the solar flux at the wavelength,  $\mathbf{I}$ , of the instrument,  $\mathbf{DI}$  is the instrument bandpass,  $\mathbf{b}_{aer}(\mathbf{I}, s)$  is the aerosol extinction coefficient,  $P(\mathbf{I}, \mathbf{J}, s)$  is the phase function, and  $\mathbf{J}$  is the scattering angle. This equation assumes that extinction from the sun to the point of scattering and from the point of scattering to the satellite can be ignored. The total radiance at 1.27  $\mu\text{m}$  includes a contribution due to  $\text{O}_2(^1\Delta_g)$  emission. In addition, the radiances at both 1.27 and 1.87  $\mu\text{m}$  contain a small contribution due to Rayleigh scattering. The Rayleigh scattering contributions, calculated from a radiance model using neutral atmosphere number density profiles provided by the Middle Atmosphere Program (MAP), were first subtracted from the radiance profiles at both wavelengths. The radiance contribution at 1.27  $\mu\text{m}$  from  $\text{O}_2(^1\Delta_g)$  emission was then removed in the following way. Below the emission peak and above the aerosol layer, a plot of the log of the radiance vs. altitude is approximately a straight line. For each radiance profile we selected the altitude between the aerosol layer and the emission peak where the increase in radiance with respect to altitude was the largest. We then linearly extrapolated downward from that altitude. An example of the  $\text{O}_2(^1\Delta_g)$  and Rayleigh determinations is shown in Figure 1. The radiance profile with the extrapolated tail was subtracted from the original radiance profile to remove the contribution due to  $\text{O}_2(^1\Delta_g)$  emission.

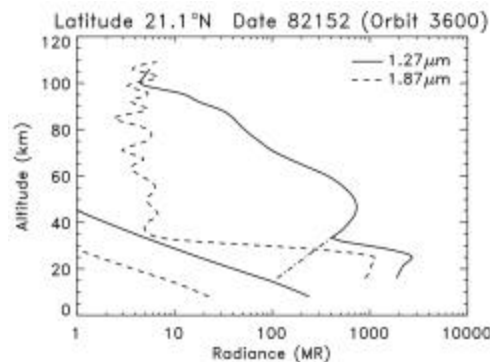


**Figure 1.** Radiances from the near-infrared spectrometer for an orbit on June 1, 1982. The upper two curves are the measured radiances, while the two curves near the lower left-hand corner are radiances due to Rayleigh scattering as calculated from a model atmosphere. The dot-dash line represents the extrapolation of the  $\text{O}_2(^1\Delta_g)$  emission in the 1.27  $\mu\text{m}$  radiance profile.

Dividing both sides of equation 1 by the solar flux gives:

$$\mathbf{t}_{aer}(\mathbf{I}) = \int_{LOS} \mathbf{b}_{aer}(\mathbf{I}, s) P(\mathbf{I}, \mathbf{J}, s) ds \quad (2)$$

where  $\mathbf{t}_{aer}$  is the slant-path optical depth due to aerosols, and the integral is calculated over the line-of-sight ( $LOS$ ). This equation can be represented by a linear matrix equation of the form

$$\mathbf{A} \mathbf{b}_{aer} = \mathbf{t}_{aer} \quad (3)$$

Here the transformation matrix,  $\mathbf{A}$ , includes the effect of atmospheric refraction as well as a complete instrument function for the near infrared spectrometer. This instrument function includes the spectrometer slit function, the tilt of the field of view with respect to the horizon, and the rotation of the satellite during the integration period for each radiance sample. A significant portion of the third-year effort was devoted to including these effects in the inversion algorithms.

Since the instrument function results in contributions to the observed radiance profile from points above and below the field of view, the solution vector,  $\mathbf{b}_{aer}$ , will have more elements than the vector of slant-path optical depths  $\mathbf{t}_{aer}$ . Thus, equation 3 is underdetermined. By adding smoothness constraints, this equation can be transformed into an overdetermined matrix equation for which there is a least-squares solution. After running numerous test cases, we concluded that internal consistency required that we implement a weighted least squares with smoothness constraints, and this is the method used in the final inversion algorithm. Figure 2 shows an example of the conversion from slant path optical depth to phase-modulated extinction for both the 1.27 and 1.87  $\mu\text{m}$  channels.

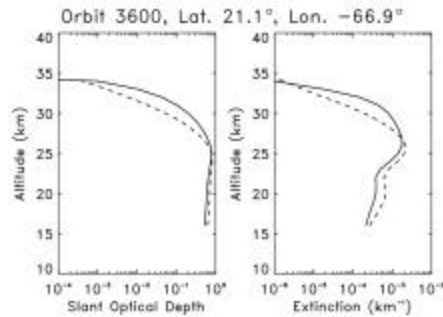


**Figure 2.** Aerosol slant-path optical depth and extinction from an orbit on June 1, 1982. The solid lines are for the 1.27  $\mu\text{m}$  channel of the near-infrared spectrometer, while the dashed lines are for the 1.87  $\mu\text{m}$  channel.

Using a constant value for the aerosol size parameters  $r_g$  and  $S$ , we converted the phase modulated extinctions to extinction coefficients for all SME measurements. A comparison of the 1.27- $\mu\text{m}$  extinctions from SME and the extinctions from the SAM II instrument is shown in Figure 3, revealing excellent agreement between the two instruments.

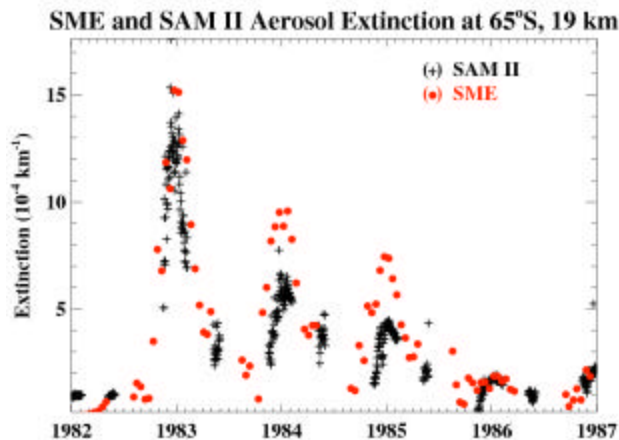


**Figure 3.** Comparison between SAM II and SME aerosol extinction at 65°S and 19 km.

The Stratosphere Aerosol and Gas Experiment (SAGE) II offers another opportunity for correlative measurements. Although SAGE was not launched until late 1984, its observations cover latitudes from 80°S to 80°N, unlike SAM II, which only made measurements at high latitudes. Figure 4 shows the SME/SAGE II aerosol extinction comparison at a latitude of 30°N at 20 km. These comparisons include only the decaying aerosols from El Chichon, but again, the agreement is very good.

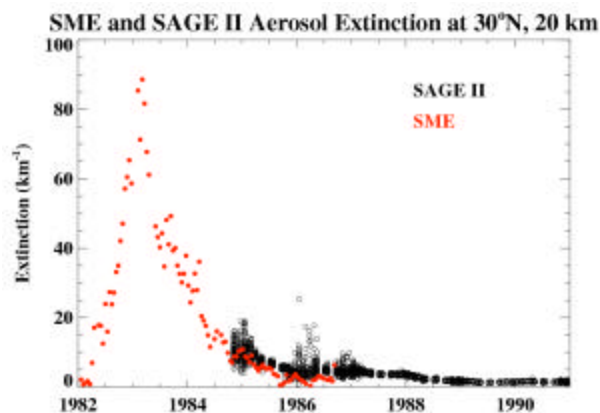


**Figure 4.** Comparison of SME 1.27- $\mu\text{m}$  and SAGE II 1.02- $\mu\text{m}$  aerosol extinction at 30°N and 20 km altitude.

Comparison of SME 1.27- $\mu\text{m}$  1.02- $\mu\text{m}$  aerosol extinction at

Figure 5 shows the evolution of SME aerosol extinction at 20, 22 and 25 km before and after the eruption of El Chichon, as a function of latitude. The cloud was largely contained in the northern hemisphere, although small increases in extinction are also observed in the southern hemisphere, primarily at equatorial latitudes. It is clear that these data will be very valuable for climate studies.

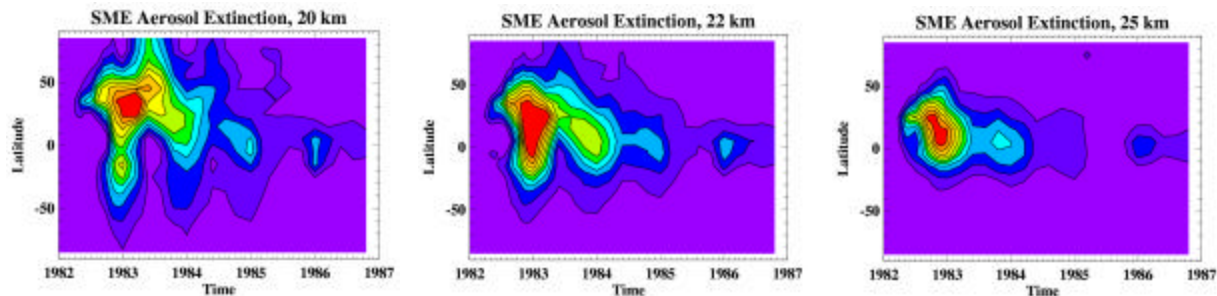


**Figure 5.** Aerosol extinction derived from 1.27- $\mu\text{m}$  SME measurements at 20, 22 and 25 km.

A paper is currently in preparation for submission to the Journal of Geophysical Research that details the inversion algorithm, the validation results, and the derived aerosol extinction morphology. As part of this preparation, the extinction calculations (conversion from phase-modulated extinction to actual extinction) are being refined to include altitude- and time-dependent aerosol size parameters. After the review process, these data will be available for use in global climate models, thus achieving the original goal of this program.

#### D. References

Eparvier, F.G., D.W. Rusch, R.T. Clancy, and G.E. Thomas, Solar Mesosphere Explorer satellite measurements of El Chichón aerosols. 2: Aerosol mass and size parameters, *J. Geophys. Res.* 99, 20,533-20,544, 1994.

Callan, M.T., C.E. Randall, D.W. Rusch and F.G. Eparvier, Aerosol Extinctions Derived from Solar Mesosphere Explorer Satellite Data, GACP science team meetings, NY, NY, September, 1999, and October, 2000.

Callan, M.T., C.E. Randall, D.W. Rusch and F.G. Eparvier, Aerosol extinctions derived from Solar Mesosphere Explorer satellite data, in preparation for submission to the Journal of Geophysical Research, 2002.